Ulrich E. Klotz, Dario Tiberto and Franz Held
fem Research Institute for Precious Metals and Metals Chemistry

Dr. Ulrich E. Klotz is Diploma Engineer in Physical Metallurgy (University of Stuttgart, Germany) and holds a PhD in Materials Science from ETH Zurich, Switzerland. He is Head of the Department of Physical Metallurgy at the Research Institute for Precious Metals & Metals Chemistry (fem) in Schwaebisch Gmuend, Germany.

The present paper describes the results of a collaborative research project on the selective laser melting of 18-karat gold alloys. Three main objectives were pursued during the project: (1) to analyze the effect of the process parameters, (2) to investigate the role of powder treatments and alloy composition and (3) to identify design rules for additively manufactured jewelry items. The laser power, the layer thickness, the scan rate and the overlap of the scans were optimized in order to reduce the porosity of the parts built in 18K yellow-gold alloy. The production of defect-free parts in gold, silver or copper alloys is challenging due to their high thermal conductivity and their high reflectivity for the infrared laser light. Therefore, the alloy powder was slightly oxidized to form a partial oxide layer of several tens of nm thickness. A significant reduction of porosity was achieved with the oxidized powders compared to the untreated powder. Another way to reduce the reflectivity and the thermal conductivity of the powder is the alloying with certain elements. A series of alloys that contained additions of Fe, Ti or Ge showed reduced reflectivity and thermal conductivity.

“Additive Manufacturing of 18-Karat Yellow-Gold alloys”

Ulrich E. Klotz, Dario Tiberto and Franz Held
fem Research Institute for Precious Metals and Metals Chemistry

1 INTRODUCTION

Additive manufacturing, colloquial also known as 3D printing, is a wide field with many different technologies and materials ranging from polymers to metals and ceramics [1]. The additive manufacturing using lasers as a heat source finds increasing interest in the jewelry and watch industry as demonstrated by the recent presentations on the Santa Fe Symposium [2-10]. Several manufacturers provide machines for the direct metal additive manufacturing. The technology is known under different names such as selective laser melting (SLM™), Direct Metal Laser Sintering / Melting (DMLS / DMLM) or LaserCUSING®. In the present paper a Concept Laser MLab80R machine was used. The powder is applied by a rubber wiper on a build platform of 50x50 or 90x90mm with 15-25µm layer thickness. The maximum power of the infrared Nd:YAG fiber laser is 100W (wavelength 1064nm).

The scope of the project was to optimize the process parameters for the present machine type for a standard yellow gold alloy (750Au-125Ag-125Cu). Each manufacturing technology has inherent design limits. In additive manufacturing it is often claimed that current design limitations can be overcome, but there are new design limitations. Such design limitations were therefore considered. The parameter study focused on parameters of the surface quality of the parts and their porosity. However, the optimization of the machine parameters is not sufficient to achieve defect free parts with good surface quality. Powder treatments were necessary in order to reduce the reflectivity of the alloy. This resulted in a significant reduction of porosity. The porosity could be further reduced by additions of additional alloying elements. Finally, surface finishing techniques were tried out in order to obtain a polished finish comparable to conventionally manufactured jewelry items.

2 ALLOY AND POWDER PROPERTIES

2.1 Reflectivity, electrical and thermal conductivity

The laser sources in in selective laser melting machines are mostly Nd:YAG lasers with a wavelength of 1064nm. While iron, aluminum, palladium and platinum show the relative low reflectivity of 60-70% at this infrared wavelength gold, silver and copper show nearly total reflectivity (Figure 1). Most of the laser energy is therefore reflected and these metals are difficult to melt despite their low melting temperature. As a result the melt pool is very small and the process window for gold alloys is much narrower compared to steel or titanium alloys [11].

The scope of alloy development will be to reduce the reflectivity in order to increase the absorbed laser energy. The thermal conductivity should also be reduced to avoid a quick dissipation of the absorbed energy. Reflectivity, electric conductivity and thermal conductivity of alloys are related to each other. The reduction of the electric conductivity and the effect on the laser melting results will be described later.

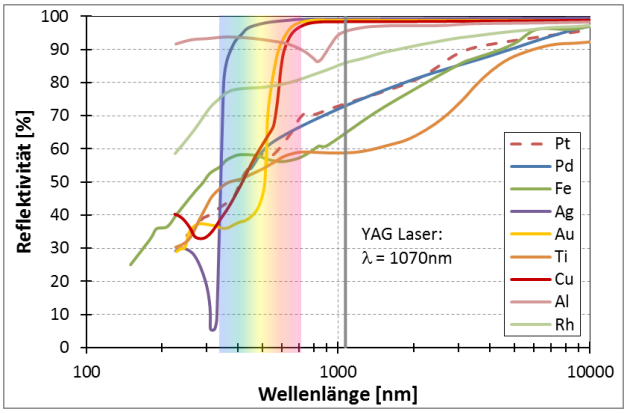

Figure 1:Reflectivity of some metals as a function of wavelength.

2.2 POWDER PROPERTIES

The properties of the alloy powder are mainly determined by their size distribution and the powder shape. A size range from 10-30µm is considered ideal for the particular machine used in this study. The powder was provided from different manufacturers and obtained by gas atomization. However, details of the manufacturing process were not disclosed. A certain particle size distribution is derived from the atomization process, and that requires the separation of the useful particle size range [12]. Sieving is used to separate the coarse particles and gas classification for the separation of the fine ones. The different powders were analyzed in the scanning electron microscope (SEM) as shown in Figure 2. The gas classified powder batch shows a narrow distribution of spherical particles. Some residues of broken, irregular particles are found. The second powder batch that was not gas classified has similar maximum particle size. However, it also contains many small particles with a size well below 10µm. Both powders were intended for the laser melting process in different machines on the market. However, in the particular machine used in this study, the processing of powder batch #2 could not provide a smooth powder bed that is required for defect free parts (Figure 3). It was found out later in the study that the flowability of the powder could be significantly improved by a powder treatment process. However, the MLabR machine seems to require powder with a lower particle size limit of around 5µm and an upper limit of ca. 40µm.

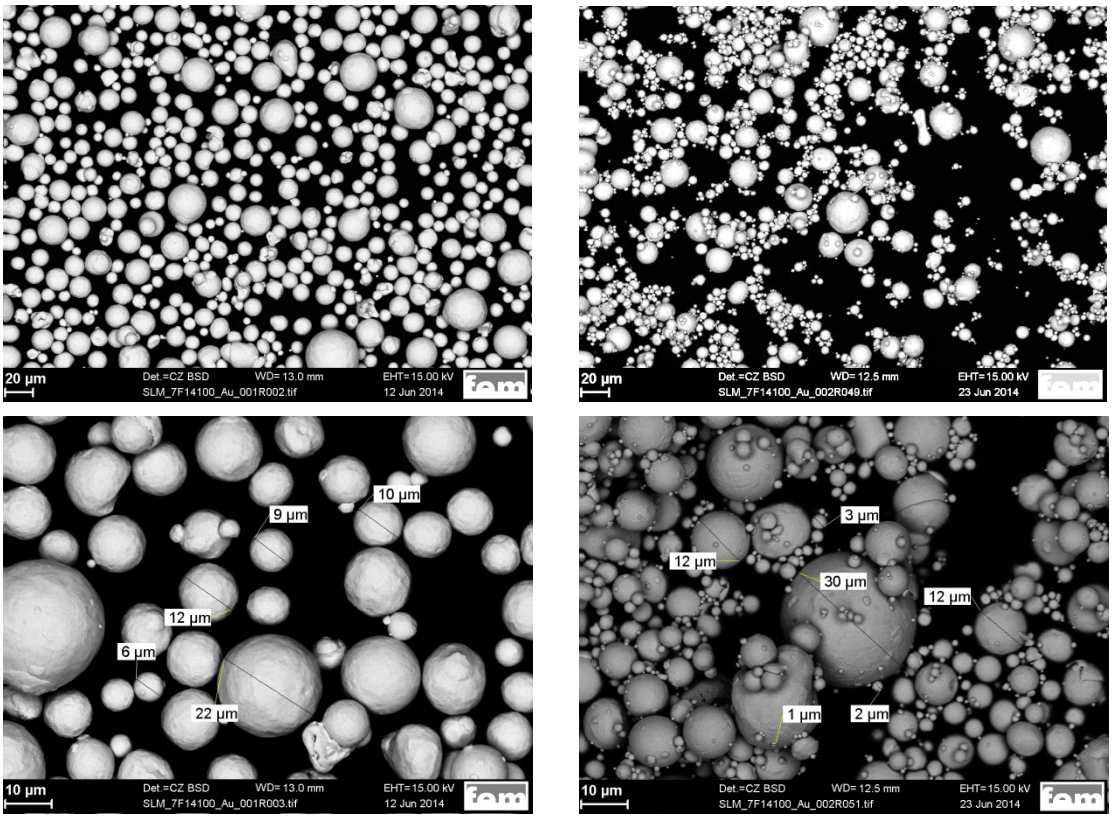

Figure 2: SEM images of the powders used in this study. Left: powder fraction #1 with gas classification, powder size 10-30µm. Right: powder fraction #2 without gas classification, powder size >30µm.

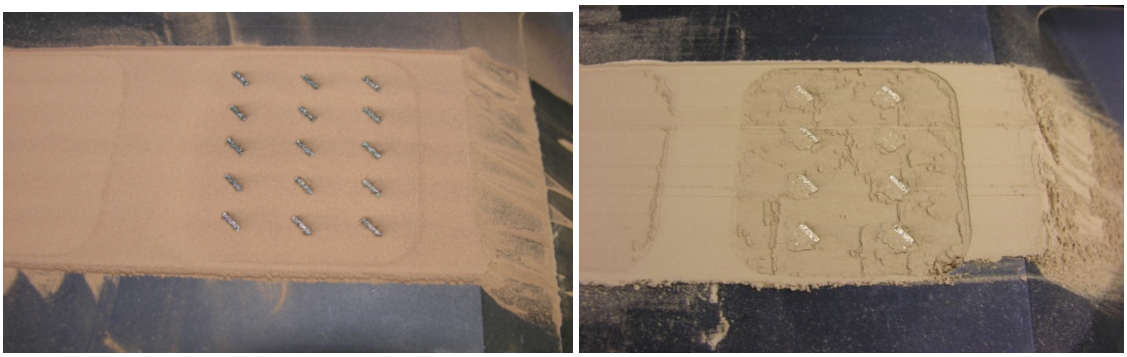

Figure 3: Smooth powder bed for powder fraction #1 (left) and rough powder bed for powder fraction #2 (right).

3 DESIGN ASPECTS

In any manufacturing technology there are limitations to the design of the products that can be produced by that particular technology. Additive manufacturing is promoted to exceed such limits, which is definitely true, but there are other limitations that have to be considered. Such limitations are the support structures of the parts. Especially in precious metals supports should be reduced as much as possible. Some design guidelines for additively manufactured jewelry parts are described in literature [3, 4, 13].

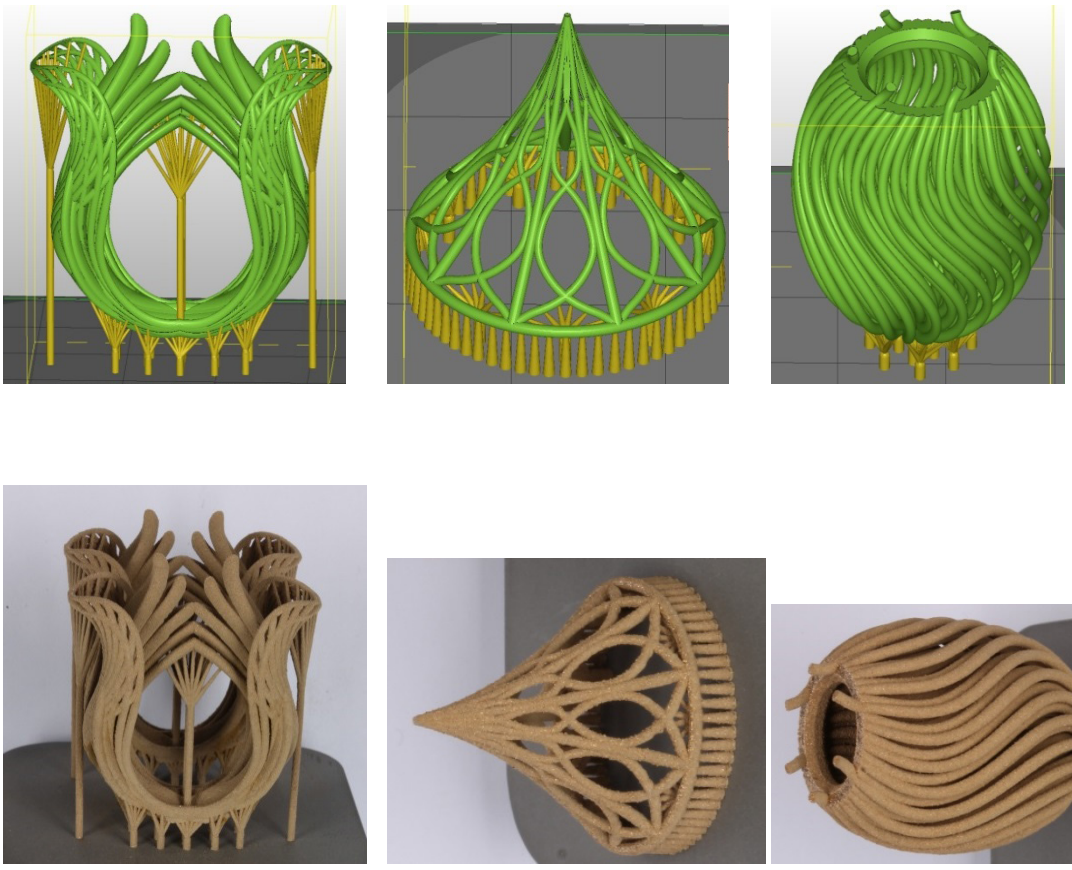

Figure 4: Upper line: Design examples provided by project partners. Left: LC Köhler, center: Janine Rall, right: Klaus Zimmermann. Lower line: designs built in Cu-10Sn bronze alloy.

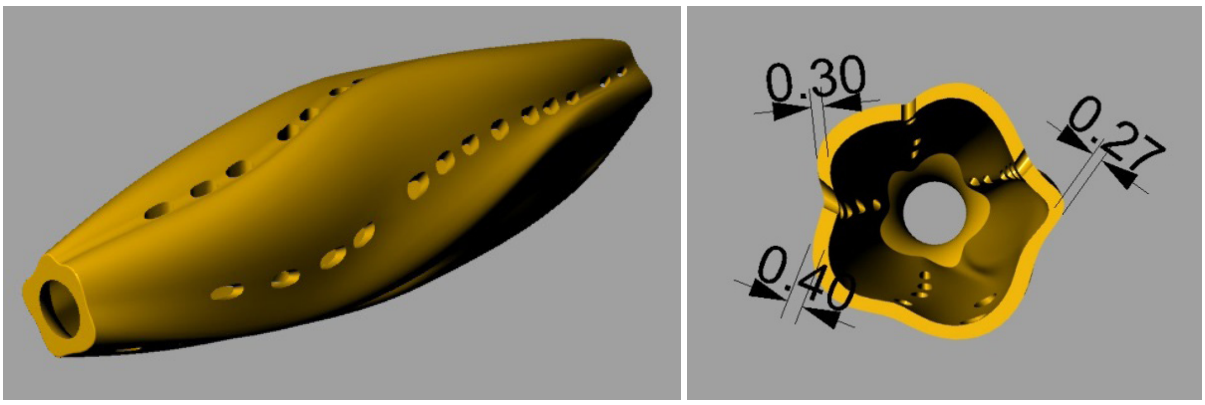

Figure 5: Design example provided by Klaus Zimmermann with dimensions in mm.

In order to consider such guidelines designers were invited to take part in the study and to provide there design examples. Some of them are shown in Figure 4. These designs consider the minimization of support structures by a selection of the correct angles between the part and the build platform (larger than 45°) and exploit the technology to build filigree wire parts that are difficult to cast. Especially the egg shaped design used these advantages. However, such filigree parts are difficult to be polished, especially

the internal parts of the wires. Other designs, such as the one shown in Figure 5 therefore use flat surfaces. This allows quite easy conventional polishing combined with thin walls and complex geometry. The progress of the additive manufacturing will surely require a close cooperation between designers and producers in order to fully exploit the potential of the technology and to avoid design that are impossible to be build [14].

4 PROCESS PARAMETER STUDIES

The most important process parameters are the scan speed and the hatch distance, i.e. the overlap of two parallel laser scan lines. The laser power and the laser spot size were set to a constant value of 95W and 30µm, respectively, in most tests. For the chosen spot size the width of a laser trace was ca. 90µm. The process parameter study was performed using a test part according to Figure 6. After the test the porosity of the part was determined on metallographic sections of the bottom plate of the test part using image analysis (Figure 7). The porosity is determined by measuring the area fraction of the pores which is equivalent to the volume fraction.

The metallographic preparation requires due diligence. The pores in additively manufactured parts are in the range of the particles size, i.e. 5-30µm, and the gold alloys are relatively soft, typically 130-160HV1. Such small pores can be smeared over during grinding and polishing, which would results in a wrongfully low porosity. The polishing quality is therefore of utmost importance for the detectable porosity level. This is illustrated by two metallographic preparations of the identical sample (Figure 8). The left image was taken after a correct polishing of the sample where the pores are clearly visible. If the pressure on the sample during grinding and polishing is too high the soft material smears over the pores and closes them. The sample looks like, if it would be free of pores. Three sections were made on each parts and the porosity reading from image analysis were evaluated altogether to obtain good statistics and reliable values of porosity. The typical scatter of the given porosity levels is ±0,2%.

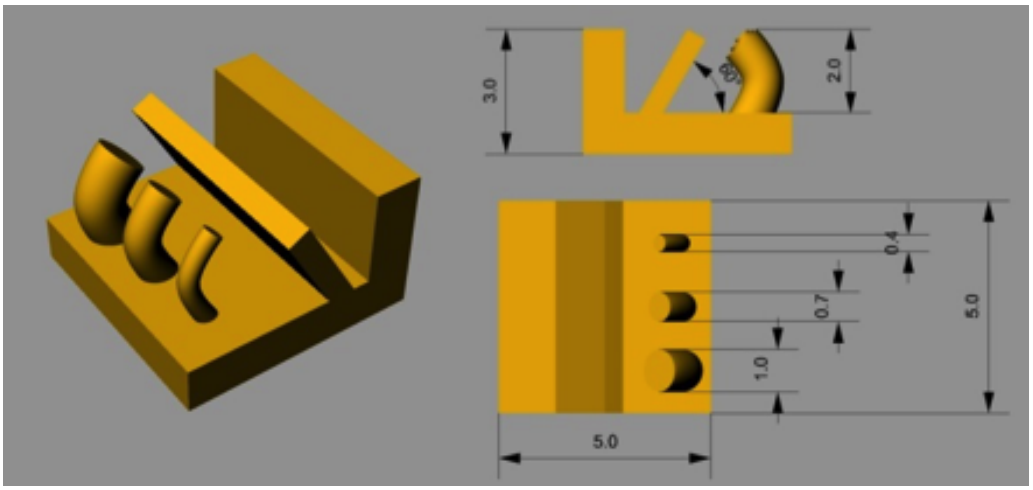

Figure 6: Test part geometry and dimensions

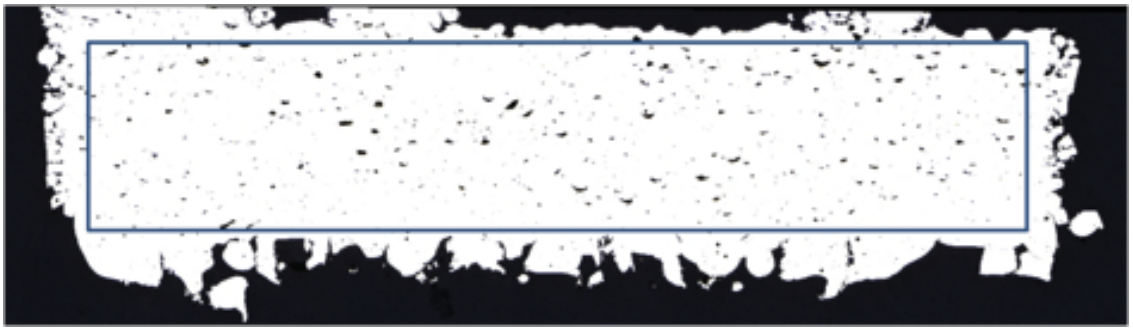

Figure 7: Rectangular area for porosity determination by optical microscopy and image analysis

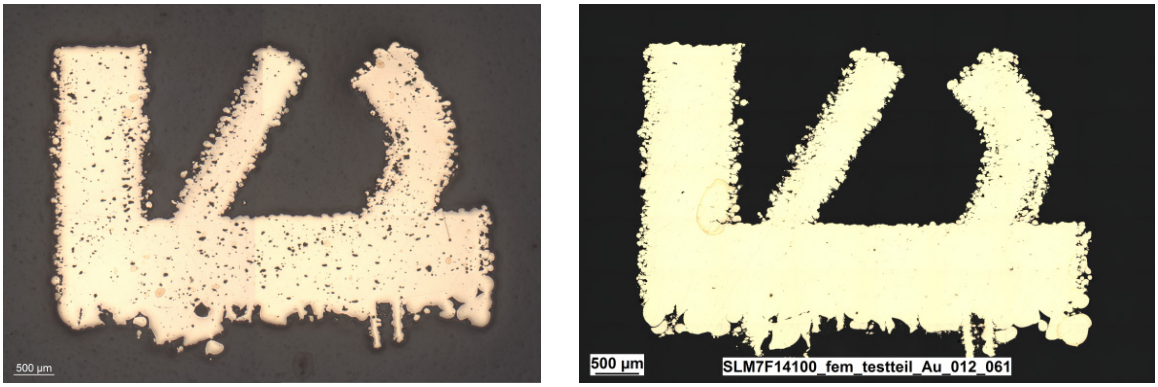

Figure 8: Effect of polishing quality on the visibility of porosity. Both images are taken on the same sample. Left: correctly polished sample. Right: Improper polishing closes the pores.

Two sets of machine parameters have to be distinguished. One parameter set is used to scan the surface of the part (“contour scan”) and another one for the bulk of the part (“hatch scan”). The sequence of scanning, i.e. bulk before surface or vice versa has a significant influence of the surface quality. In a first step of the study the bulk parameter were optimized with the objective of an ideally fully dense part free of any pores. In a second step the parameters for the surface and the sequence of scanning was optimized.

5 HATCH SCAN PARAMETERS

5.1 Untreated powder

The initial tests were done with as-received, air-dried powder. The porosity was determined as a function of the laser scan speed as shown in Figure 9. Very high porosity and a very large scatter were observed for the untreated powder. With increasing scan speed the porosity is becoming smaller, but even the best samples show values of about 3%. Figure 10 shows metallographic pictures of the untreated powder for two scan speeds. For a low scan speed the pores are very large and the layers are not completely welded together. For the higher scan speeds the pores are much smaller and the pore size distribution is narrower. The effect of scan speed on porosity can be explained with the metallographic pictures. At the low scan speed the scanned surface is very wavy, because the material tends to ball [11]. Such waviness is much larger than the applied powder layer (30µm) and therefore voids remain between the layers of molten metal. In case of a higher scan speed the melt pool is elongated and the balling tendency is reduced. The flatter surface allows a complete coating with the subsequent powder layer. A very flat surface after is therefore mandatory for a reduced porosity. For the particular setup in this study a laser scan speed of min. 150mm/s is required to reach satisfactory porosity levels. At scan speed exceeding 500mm/s the porosity starts to slightly increase again (blue curve in Figure 9) because the energy input per unit length becomes too low for a continuous melt pool.
The hatch distance is defined as the distance of two parallel scan lines. The tests showed that it plays an important role for the final porosity. In case of a small hatch distance (large overlap of two scan lines) the porosity is very high, probably because most of the laser energy is reflected from the already melted surface. In case of a high hatch distance the overlap of the layers can be too small to completely weld two parallel scan together. Hatch distances between 54µm and 27µm were tested and optimum values were obtained for a hatch distance of 36µm.

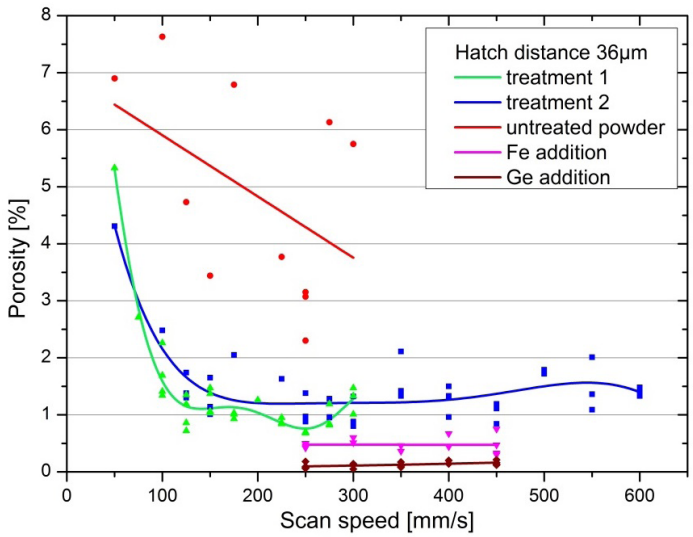

Figure 9: Effect of the scan speed on the porosity for different powder qualities.

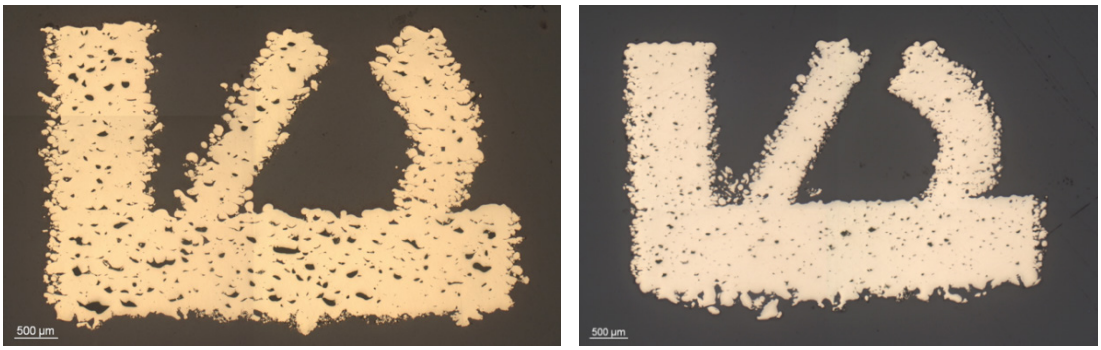

Figure 10: 18k yellow gold samples with two sets of parameters. Left: v = 50mm/s, hatch distance 27µm, resulting porosity 7%. Right: v = 250mm/s, hatch distance 36µm, resulting porosity 3,5%.

In summary, for the untreated powder the porosity level is still much too high. The strength of the parts produced in these initial tests is very low and quality of the part is unacceptable for the untreated powder. As a consequence the powder must be treated somehow to reduce its reflectivity. Such powder treatment and modifications are described in the following sections.

5.2 Powder treatment

The scope of the powder treatment was to reduce the surface reflectivity in order to increase the amount of laser energy that is absorbed by the sample. The spectral reflectance of silver coatings was investigated in [15]. The authors of that study found that the reflectivity of the silver surface was reduced significantly by a by a sulfidation process, something that is well known in jewelry industry as tarnishing. However, in the infrared range (λ=1000nm), the reflectivity was reduced by a factor of four compared to green light (λ=500nm). Similar results were found for copper oxide layers [16]. Based on this information, a suitable treatment process was elaborated.

The effect of such treatment on porosity is demonstrated in Figure 9. Figure 11 shows the related microstructure images. After the treatment the porosity significantly decreases below 1,5% for scan speeds above 100mm/s and then remains constant. Taking into account the scatter of the different samples a porosity of about 1% is obtained repeatedly. The positive effect of the powder treatment was observed for different hatch distances. With the machine used in this study the lowest porosity was obtained for a hatch distance of 36µm. Another positive effect of the powder treatment is the improvement of the flowability of the powder. Especially powders with some fine fractions that are poorly flowing benefit from the powder treatment.

The metallographic cross sections show the porosity and the distribution of the pores inside the parts (Figure 11). Other interesting information is the roughness of the side wall and the top surface of the part. The top surface represents the laser melted surface that shows a certain roughness as shown in Figure 16. The unevenness of this surface is one source of the porosity in the final part. The uneven surface has to be filled by powder particles that are applied in the next layer, something that can be difficult, if the surface becomes very uneven. To achieve an even surface is therefore mandatory to further reduce the porosity. An even surface requires that the melt remains liquid for a longer time so that it is possible for the surface to flatten by the flowing melt. This means the absorbed energy has to be further increased or that the energy absorbed by the sample should dissipate more slowly. One way to achieve this is a modification of the alloy composition.

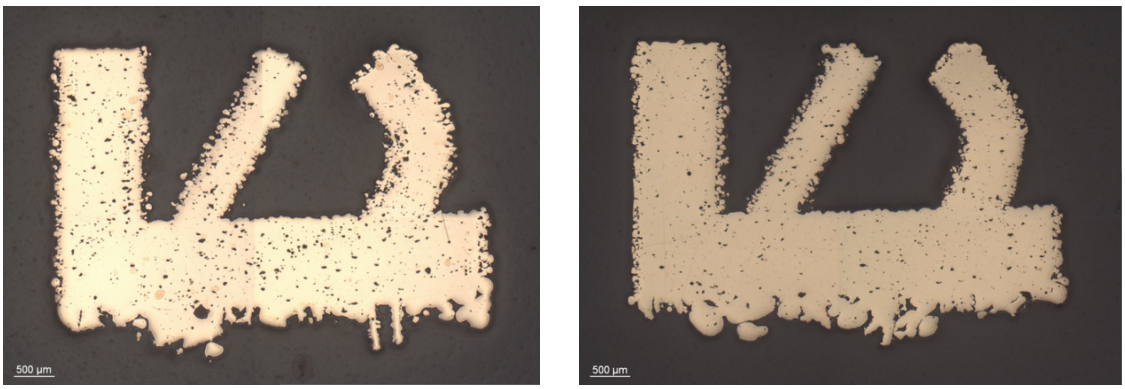

Figure 11: 18k yellow gold samples with two sets of parameters. Left: v = 150mm/s, overlap 50%, resulting porosity 1,5%. Right: v = 250mm/s, overlap 60%, resulting porosity 0,7%.

ALLOY MODIFICATION

Selection of alloying elements

The scope of the alloy modification was to reduce the thermal conductivity and the reflectivity in order to increase the absorbed laser energy. The solid solution of alloying element is well known to reduce the electric conductivity. The electric and thermal conductivity of metals and alloys is directly coupled by Lorenz number L in the Wiedemann-Franz law [17]. The effect of various alloying elements on the electric conductivity of pure gold can be found in reference books (Figure 12). According to the data for pure gold titanium, vanadium, iron and cobalt are the most effective elements to reduce electric and thereby thermal conductivity. Germanium has a similar effect and also reduces the solidus temperature significantly.

Wiedemann-Franz Law $\lambda = \sigma \bullet \Lambda \bullet T$

λ: thermal conductivity σ: electric conductivity

T: temperature $L = 2{,}1 - 2{,}9 \cdot 10^{-8}\ W\Omega K^{-2}$ (Lorenz number)

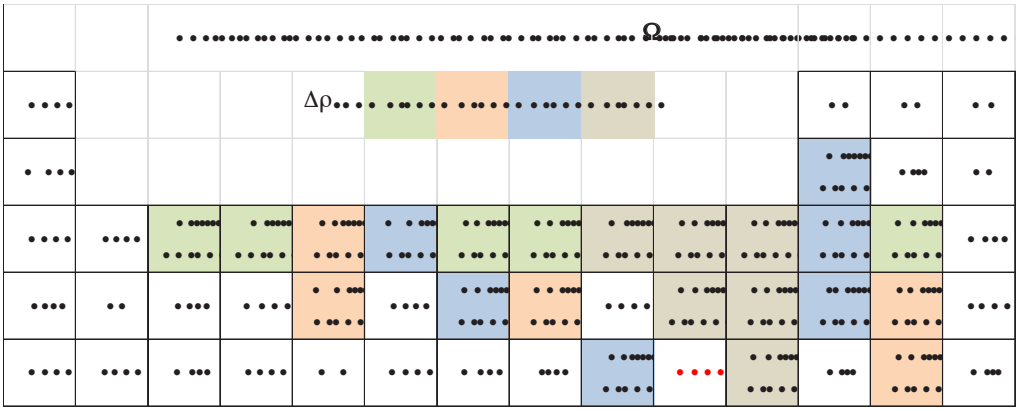

Figure 12: Increase of the electric resistance of pure gold by alloying [18].

Based on thermodynamic simulations promising alloy compositions were identified. The alloying addition was chosen to keep the elements in solid solution in order to maximize their effect. Selected alloys were prepared by melting and casting. The samples were rolled to sheet and their properties were characterized and compared to a standard yellow gold alloy (3N). The 3N alloy shows a significantly lower electric conductivity than pure gold because of the copper and silver in solid solution (Figure 13). The additional elements show a further reduction with the strongest effect for titanium and vanadium. Germanium and iron have a moderate effect that increase with increasing content (series Fe001 to Fe003).

The spectral reflectance was measured using an Avantes AvaSpec-2048 spectrometer with a wavelength range of 200-1100nm. Figure 14 shows the effect of alloying additions to pure gold for the 3N standard yellow gold and two selected alloys. The reflectivity significantly drops by alloying, because reflectivity and conductivity are directly related by the Hagen-Rubens relation [17]. The additional alloying elements iron and germanium further reduce the reflectivity as expected from the electric conductivity results. Both alloys show a similar value, but the germanium containing alloy has a significantly lower solidus temperature.

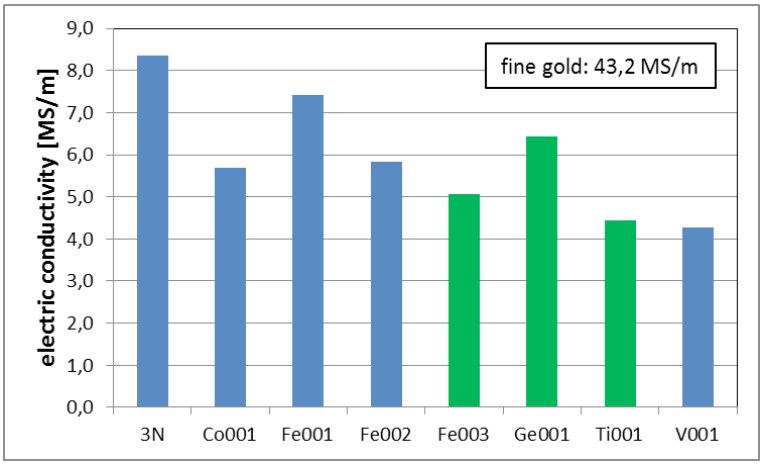

Figure 13: Electric conductivity in Mega Siemens per meter (MS/m) of a standard yellow gold alloy (3N) and of alloys with additions of Co, Fe, Ge, Ti and V. For comparison: the electric conductivity of titanium is ca. 1MS/m.

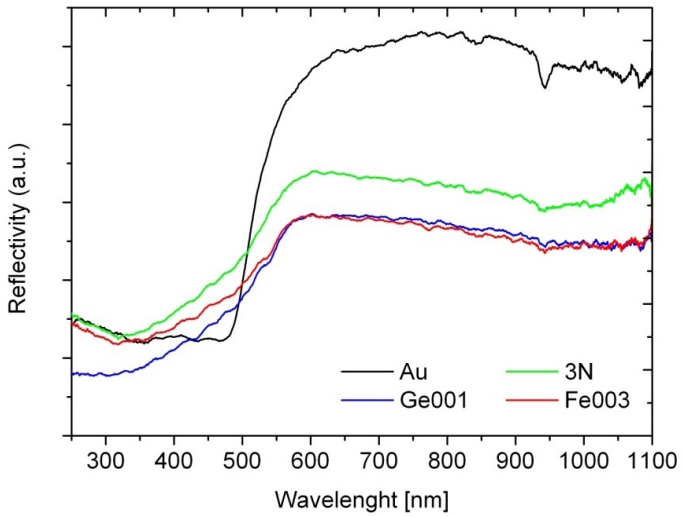

Figure 14: Spectral reflectance of gold compared to standard yellow gold (3N) and the modified alloys.

6.2 LASER MELTING RESULTS USING MODIFIED ALLOYS

The germanium and iron containing alloys were chosen for further tests. 3000 grams of each alloy was atomized by one of the project partners which resulted in useable powder of about 1500g. The titanium containing alloy shows even lower conductivity, but this alloys was too reactive to be atomized. For the iron and germanium alloy the porosity was again investigated as a function of the laser parameters. Results of the porosity as a function of scan speed are shown in Figure 9. Compared to the treated standard alloy powder a further significant reduction of porosity could be achieved. The scatter of the porosity values was also reduced. In the investigated range the porosity is independent of the scan speed.

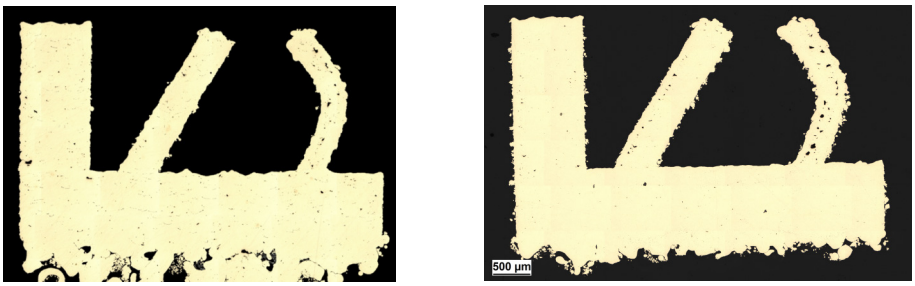

Figure 15: Porosity of modified gold alloys for the same laser parameters. Left: Fe containing alloy; 0,3% porosity.
Right: Ge containing alloy; 0,1% porosity.

The metallographic images show the pore distribution in the entire part (Figure 15). A significant reduction of porosity was achieved by alloying. In both cases the porosity is well below 0,5% and therefore comparable to investment cast parts. As discussed above the reason for the reduced porosity is the reduced laser reflection, the lower thermal conductivity and in case of the Ge containing alloy, the wider melting range. This combination of properties allows higher energy absorption and slower heat dissipation. As a consequence the melt pool stays liquid for a longer time and is elongated along the direction of the laser movement. Figure 16 shows SEM images of the laser scanned surface for different alloys. The hatch scanned surface of the treated standard alloy shows certain waviness that is responsible for porosity of the part as described above. By the modification of the alloy composition the hatched surface becomes much less wavy. Balling is reduced, the surface is flatter and the porosity is reduced.

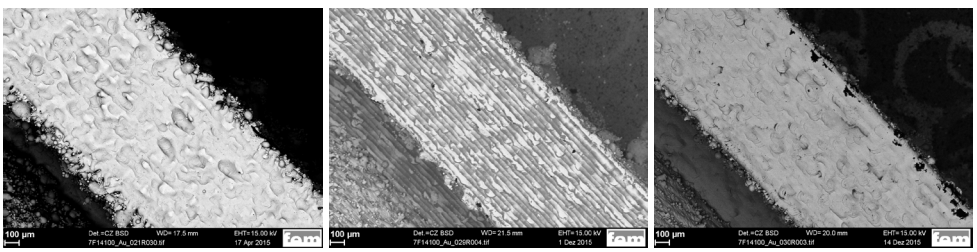

Figure 16: Surface of laser melted parts with smooth laser scanned surface. Hatch scan speed 250mm/s, hatch distance 36µm.
Left: Treated standard alloy, porosity 1,1%. Center: Fe alloyed powder, porosity 0,4%. Right: Ge alloyed powder, porosity 0,1%.

The measurement area for porosity is the bottom plate of the part as described in Figure 7. It appears that the porosity is higher in the parts sticking out of the bottom plate. In the curved wire this is an effect of the position of the metallographic plane. For the vertical and the inclined part the scanning strategy causes some subsurface porosity. At the edges of the part the laser changes its direction as shown in Figure 15. The vertical surfaces of the part are therefore scanned twice: at first by the contour scan and secondly by the hatch scan. Therefore the edges of the part are always protruding from the hatch surface a bit. These “side walls” of the samples have a width of about 100µm. The trenches behind these side walls are a bit deeper than the waviness of the rest of the hatched surface. As described above, such dimples or trenches on the surface are a source of pores. As a consequence the risk of pores is higher in a depth of ca. 100µm below the surface. During finishing such pores might show up, if too much material is removed during polishing.

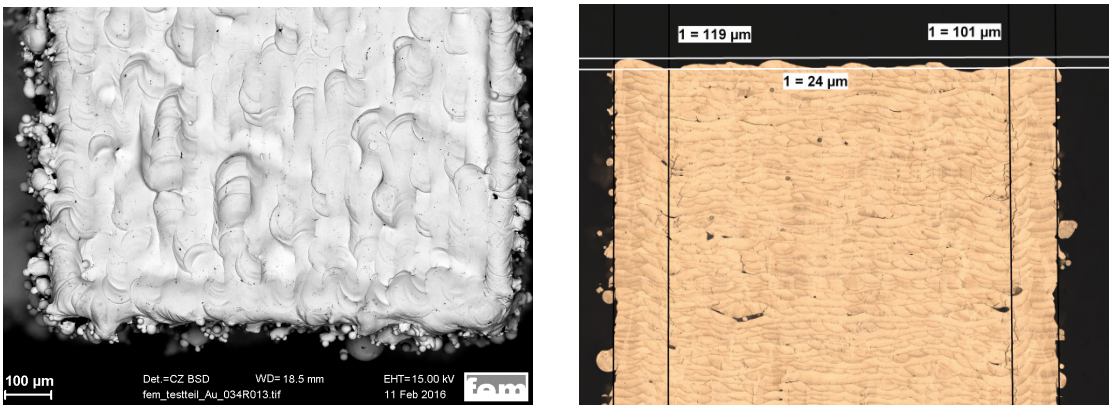

Figure 17: Origin of sub-surface porosity. Left: SEM image of the surface showing contour scan and hatch scan (test Au34_A2). Right: metallographic section indicating the width of the contour scans and the waviness of the hatch scanned surface (test Au30_A3).

7 CONTOUR SCAN PARAMETERS

The results shown so far focused on the hatch parameters of the interior of the part with in order to reduce porosity. The surface quality of the part can be optimized by the contour parameters and the sequence of the contour and the hatch scan. Figure 18 demonstrates the effect of contour parameters on the surface roughness. The poorest surface quality is obtained for a slow contour scan following the hatch scan. Increasing the scan speed significantly reduces the surface roughness. Contour scan speeds up to 1200mm/s were tested. A speed of 600mm/s represents an optimum value. For higher scan speeds the surface roughness slightly increases. The high surface roughness is caused by powder particles that are sticking to the surface, either by partial melting or sintering. The lower the scan speed the higher the heat dissipation to the powder bed and the more particles are sticking to the surface.
In the first tests the contour scan was done after the hatch scan. This resulted in a poor surface quality. The reason for that is the relatively low scan speed of the hatch scan. The following contour scan cannot improve the surface quality significantly. However, if the contour scan is done prior to the hatch scan the surface roughness was significantly reduced. In this case the contour scan is surrounded by powder on either side that has a low thermal conductivity. Less powder particles are sticking to the contour, if the speed is sufficiently high. The following hatch scan cannot deteriorate the surface.

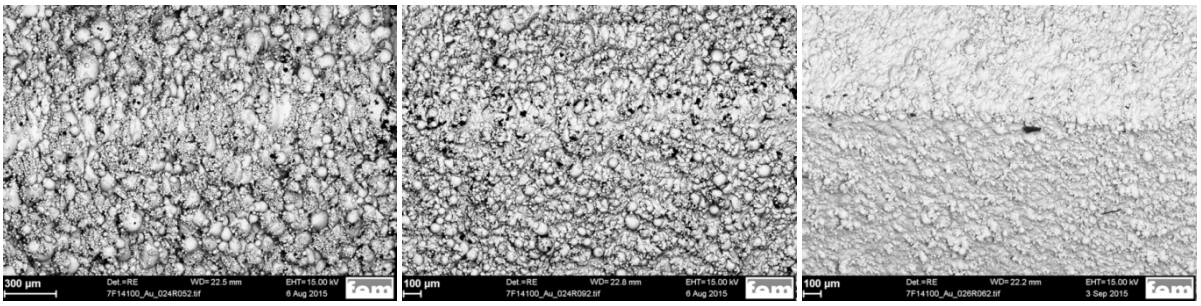

Figure 18: Effect of contour parameters on the surface roughness. Left: slow scan speed (20mm/s), contour scan after hatch scan. Center: medium scan speed (600mm/s), contour scan after hatch scan. Right: medium scan speed (650mm/s), contour scan before hatch scan.

A careful observation of the surface shows that the porosity is different on the different faces of a sample. The powder is applied by a rubber wiper from one side. The surface facing towards the wiper is always slightly rougher, i.e. more powder particles are sticking to this surface, than the surface on the opposite side. In order to assess the surface quality a cylinder with 5mm diameter was build using the optimum process parameters described above with a treated standard alloy powder. The roughness was measured on the side facing towards the wiper and on the opposite side (Table 1). The origin of such roughness difference is supposed to lie in the way the powder is applied. The rubber wiper pushes the powder towards the sides of the part that face towards the wiper. The contact between powder and part is therefore close. On the opposite side the rubber wiper snaps over the "side walls" of the sample that caused by the contour scan. This results in a slight gap between the part and the powder bed. In the following laser scan the thermal contact between powder and part is better on the wiper side compared to the opposite side. This results in more powder sticking on the wiper side and as a consequence a rougher surface of that side.

Table 1: Surface roughness as a function of sample orientation relative to the wiper and in different surface finishing conditions. R_a is the arithmetic average of the absolute values. R_z is the average distance between the highest peak and lowest valley in each sampling length. The tital sampling length was 12.5mm that was divided in five segments for the determination of R_z.

	Wiper side		Opposite side	
Position	**Ra [µm]**	**Rz [µm]**	**Ra [µm]**	**Rz [µm]**
As manufactured	12,9	77,9	10,1	62,9
Sand blasted using 120-200µm corundum	5,5	37,6	3,8	25,3
Blasted using 120-200µm plus 50µm corundum sand	4,7	31,3	3,0	19,4
Blasted using 120-200µm plus 50µm corundum sand plus 50-100µm glass beads	4,2	24,3	3,1	19,0
Blasted using 120-200µm plus 50µm corundum sand plus 25µm glass beads	4,2	25,1	2,7	17,9

8 SURFACE TREATMENT

The surface treatment of the as-build parts included several steps. Ultrasonic cleaning was used to remove loose powder particles. Figure 19 shows this condition labelled "as manufactured". The surface roughness consists of particles that are loosely sintered or have welded to the surface. Such particles can be removed quite easily by sand blasting. Depending on the size of the corundum sand the surface shows a level of roughness that is caused by the mismatch of the different metal layers. To flatten this roughness peening with glass beads is effective. This deforms the surface layer and increases the surface hardness. Excessive peening should be omitted to avoid bending of the part by the induced residual stresses. Figure 19 shows the effect of different surface treatment processes, depending on the size of the used sand. After the blasting and peening processes the surface was electro polished or hand polished. Some jewelry parts are shown in Figure 20.

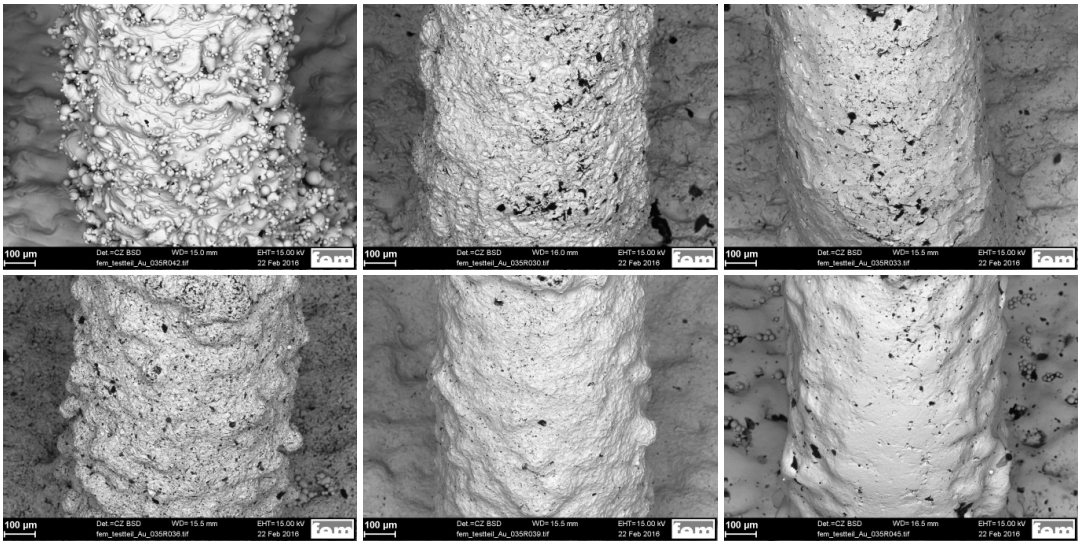

Figure 19: Surface after different processing steps (from left to right): as manufactured, sand blasted with 120-200µm corundum, as before plus blasting with 100-200µm glass beads, sand blasted with 50µm corundum, as before plus blasting with 25µm glass beads, as before plus electro-polishing.

Figure 20: Jewelry samples in standard yellow gold in the different polishing steps. From left to right: as-manufactured, sand blasted, electro polished, hand polished

9 SUMMARY AND CONCLUSIONS

A process study on the additive manufacturing of yellow gold alloys using a ConceptLaser MLab80R LaserCusing machine was conducted. The main results of this work are:

The optimum powder size is 10-30µm. The fine fraction of the powder needs to be removed to obtain a smooth powder bed in the particular machine used in this study.

The laser speed of the hatch scans is the most important parameter to reduce the porosity. The optimum laser speed is in the range of 200-500mm/s.

The minimum porosity using untreated, i.e. freshly atomized powder is about 2,5%. In order to reduce the porosity the powder requires a surface treatment that reduces the reflectivity of the surface and the thermal conductivity. The minimum porosity using surface treated powder is about 0,7%.

Alloying additions cause reduction of reflectivity and electrical conductivity of the alloy. This results in a further reduction of porosity to 0,3-0,1% in the best cases.

The surface roughness is influenced by the orientation of the part relative to the wiper direction. The sides of the parts facing towards the wiper show higher surface roughness.

Surface finishing includes several steps starting from ultrasonic cleaning over sand blasting and glass peening to electro or hand polishing.

10 ACKNOWLEDGEMENT

Gefördert durch:

Bundesministerium für Wirtschaft und Energie

aufgrund eines Beschlusses des Deutschen Bundestages

This work was funded by the German Ministry for Economics and Energy based on a decision of the German Bundestag via the AiF-IGF programme (No 17729N). The industrial project partners namely ConceptLaser, Ehinger-Schwarz, C. Hafner, Heimerle+Meule, Idee Schmuckideen, Indutherm Erwärmungsanlagen, Kinzel&Rall, L.C. Köhler and OTEC Präzisionsfinish are acknowledged for their support by providing precious metals, consumables and equipment .

1 References

[1] Gebhardt, A., *Generative Fertigungsverfahren*. 4th edition ed. 2013: Carl Hanser Verlag, Munich.

[2] Cooper, F. *Sintering and additive manufacturing: the new paradigm for the jewelry manufacturer*. in *The Santa Fe Symposium on Jewelry Technology*. 2012. Albuquerque, NM, USA.

[3] Cooper, F. *DMLM support: are they the jewelry industry's new sprue, riser and gate feed?* in *The Santa Fe Symposium on Jewelry Technology*. 2014. Albuquerque, NM, USA.

[4] Dean, L.T. *Creative approaches to design and manufacturing in the digital age*. in *The Santa Fe Symposium on Jewelry Technology*. 2013. Albuquerque, NM, USA.

[5] Dean, L.T. *Precious: another layer of luxury*. in *The Santa Fe Symposium on Jewelry Technology*. 2015. Albuquerque, NM, USA.

[6] Fletcher, D. *Use of emanufacturing design software and DMLS in the jewelry industry*. in *The Santa Fe Symposium on Jewelry Technology*. 2014. Albuquerque, NM, USA.

[7] Zito, D. *Laser developments in the slective laser melting production of gold jewelry*. in *The Santa Fe Symposium on Jewelry Technology*. 2012. Albuquerque, NM, USA.

[8] Zito, D. *Optimzation of the main selctive laser melting technology parameters in the production of precious metal jewelry*. in *The Santa Fe Symposium on Jewelry Technology*. 2013. Albuquerque, NM, USA.

[9] Zito, D. *Optimization of SLM technology main parameters in the production of gold and platinum jewelry*. in *The Santa Fe Symposium on Jewelry Technology*. 2014. Albuquerque, NM, USA.

[10] Zito, D. *Definition and solidity of gold and platinum jewelry produced using selective laser melting (SLM)*. in *The Santa Fe Symposium on Jewelry Technology*. 2015. Albuquerque, NM, USA.

[11] Khan, M. and Dickens, P., *Selective Laser Melting (SLM) of pure gold.* Gold Bulletin, 2010. **43**(2): p. 114-121.

[12] Fischer-Bühner, J. *Optimierte Edelmetallpulverherstellung*. 2015 [cited 2016, 1st March]; Available from: https://www.hs-pforzheim.de/De-de/Hochschule/Einrichtungen/STI/Teaser_Aktuelles/Documents/Indutherm%20Pulverherstellung.pdf.

[13] Biagi, B., *Jewels design using digital technologies*, in *Jewelry Technology Forum (JTF)*. 2016, LEGOR GROUP S.p.A: Vicenza, Italy.

[14] Adler, S. *CAD/CAM follies*. in *The Santa Fe Symposium on Jewelry Technology*. 2011. Albuquerque, NM, USA.

[15] Barrera-Calva, E., Ortega-López, M., Avila-García, A., and Matsumoto-Kwabara, Y., *Optical properties of silver sulphide thin films formed on evaporated Ag by a simple sulphurization method.* Thin Solid Films, 2010. **518**(7): p. 1835-1838.

[16] Sabbaghan, M., Shahvelayati, A.S., and Madankar, K., *CuO nanostructures: Optical properties and morphology control by pyridinium-based ionic liquids.* Spectrochimica Acta Part A: Molecular and Biomolecular Spectroscopy, 2015. **135**: p. 662-668.

[17] Hummel, R.E., *Electronic properties of materials*. 1985: Springer.

[18] Beck, G., *Edelmetall-Taschenbuch*. 2nd edition ed. 1995: Degussa AG, Frankfurt und Hüthig GmbH, Heidelberg.